






RESEARCH ARTICLE

Tall tower observations of a northward surging gust front in central Amazon and its role in the mesoscale transport of carbon dioxide

Luciane I. Reis¹  | Maurício I. Oliveira^{1,2}  | Cléo Q. Dias-Júnior^{1,3}  |
 Hella van Asperen⁴ | Luca Mortarini⁵  | Otávio C. Acevedo⁶ |
 Christopher Pöhlker⁷ | Leslie A. Kremper⁷ | Bruno Takeshi¹ |
 Carlos A. Quesada¹ | Daiane V. Brondani⁸ 

¹National Institute of Amazonian Research (INPA), Petrópolis, Manaus, Brazil

²Department of Physics, Federal University of Santa Maria, Santa Maria, Brazil

³Department of Physics, Federal Institute of Pará (IFPA), Belém, Brazil

⁴Biogeochemical Processes, Max Planck Institute for Biogeochemistry, Jena, Germany

⁵Department of Earth Sciences “Ardito Desio”, University of Milan (UNIMI), Turin, Italy

⁶School of Meteorology, University of Oklahoma, Norman, Oklahoma, USA

⁷Multiphase Chemistry Department, Max Planck Institute for Chemistry, Mainz, Germany

⁸Institute of Atmospheric Sciences and Climate, National Research Council-CNR - ISAC, Lecce, Italy

Correspondence

Luciane I. Reis, National Institute of Amazonian Research (INPA), Petrópolis, Manaus 69080971, Brazil.
 Email: luciane10reis@gmail.com

Present address

Leslie A. Kremper, Laboratory for Climatology and Remote Sensing, Department of Geography, University of Marburg, Marburg, Germany.

Funding information

German Federal Ministry of Education and Research - BMBF, Grant/Award Numbers: 01LB1001A, 01LK1602A, 01LK1602B; Brazilian Ministério da Ciência, Tecnologia e Inovação - MCTI/FINEP, Grant/Award Number: 01.11.01248.00; Amazon State University (UEA); FAPEAM; CAPES; Reserva de Desenvolvimento Sustentável do Uatumã SDS/CEUC/RDS-Uatumã (SDS/CEUC/RDS-Uatumã)

Abstract

High-frequency measurements obtained at two micrometeorological towers are investigated for a rare northward surging gust front that impacted the Amazon Tall Tower Observatory (ATTO), in central Amazon. The gust front originated from a decaying mesoscale convective system (MCS) during the morning hours of 27 December 2021 near Manaus, Amazonas state, northern Brazil, and surged north-eastward towards the ATTO site. Large temperature drops and vigorous, persistent winds were observed at the towers which lasted for over 4 h despite the gust front being detached from its parent, decaying MCS. More importantly, the gust front was responsible for drastic increases of CO₂ concentrations throughout the tower depths, which suggests that the gust front winds horizontally advected CO₂-rich air from a source upstream from the ATTO site. The CO₂-rich outflow is hypothesized to originate from downward transport and/or biomass burning from forest fires in southeastern Amazon, both ideas that are supported by large increases of aerosol concentrations measured at ATTO following the gust front passage. Our results stress the need for further investigations addressing the role played by mesoscale convective circulations in the redistribution of trace gases and aerosols in the Amazon.

This is an open access article under the terms of the [Creative Commons Attribution](https://creativecommons.org/licenses/by/4.0/) License, which permits use, distribution and reproduction in any medium, provided the original work is properly cited.

© 2024 The Author(s). *Meteorological Applications* published by John Wiley & Sons Ltd on behalf of Royal Meteorological Society.

KEYWORDS

CO₂, cold pool, convective storms, forest fires, gust front

1 | INTRODUCTION

Convective storms can engender large and sudden variations in the evolution of the kinematic, thermodynamic and chemical structure of the planetary boundary layer (PBL) (Betts et al., 2002; Dias-Júnior et al., 2017; Fitzjarrald et al., 1990; Gerken et al., 2016; Mendonça et al., 2023; Oliveira et al., 2020; Xie et al., 2022). Upon reaching maturity, convective storms produce downdrafts via latent cooling from evaporation of rain and melting of graupel/hail as well as aerodynamic drag from falling hydrometeors (Fournier & Haerter, 2019; Wakimoto, 1982). The negatively buoyant downdrafts reach the PBL and spread horizontally, producing an extensive area of precipitation-cooled air denominated cold pool. The leading edge of horizontally spreading cold pool is named gust front and is marked by sharp gradients of temperature, wind speed, wind direction, pressure (Wakimoto, 1982) and even concentration of certain atmospheric constituents (Gerken et al., 2016). Observations of gust fronts and attendant cold pools at high temporal frequency and vertical resolution are key to determine the mechanisms by which they affect the exchanges of mass, momentum and energy in the PBL (D'Oliveira et al., 2022; Fitzjarrald et al., 1990; Gerken et al., 2016; Mendonça et al., 2023; Oliveira et al., 2020; Xie et al., 2022).

In the Amazon rainforest, convective storms are nearly ubiquitous and, consequently, contribute to the frequent occurrence of downdrafts, gust fronts and cold pools (Betts et al., 2002). Often, storms in the Amazon congeal into large mesoscale convective systems (MCSs) that are responsible for as much as 50%–70% of rainfall in the Amazon basin (Rehbein et al., 2019). The occurrence of MCSs in the Amazon is frequently associated with the formation of squall lines when storms become organised into a linear arrangement composed of a leading line of convective precipitation, followed by a trailing zone of stratiform precipitation (Cohen et al., 1995; Garstang et al., 1994; Greco et al., 1994; Houze et al., 1990; Houze Jr, 2004; Pereira Filho et al., 2002). The typical and well-studied Amazonian squall line forms on the coast of the Amazon basin, travels southwestward embedded in the northeasterly flow (Bezerra et al., 2021; Cohen et al., 1995; Garstang et al., 1994; Greco et al., 1994; Melo et al., 2019) and is characterized by a large MCS as seen in satellite imagery with very cold cloud-top temperatures (Machado et al., 1998; Rehbein et al., 2019). Although the

majority of squall lines traverse the Amazon basin from the northeast, some squall lines can display a strong southerly component and typically move from the southwest (Alcântara et al., 2011; Alonso & Saraiva, 2005). Negrón-Juárez et al. (2017) have shown that, despite less frequent than northeasterly squall lines, southerly squall lines are more frequent than previously thought and are responsible for a considerable number of windthrow events. Still, the number of studies addressing southerly squall lines/MCSs in the Amazon remains small relative to northeasterly squall lines (Melo et al., 2019; Negrón-Juárez et al., 2017).

Strong MCSs and local convective storms have been shown to drastically modify the thermodynamic, kinematic and chemical properties of the PBL (Betts et al., 2002; Fitzjarrald et al., 1990; Gerken et al., 2016; Mendonça et al., 2023; Oliveira et al., 2020). Convective downdrafts can enhance the mixing of air within the forest with the overlying lower PBL, sometimes even penetrating towards the forest floor and fostering evacuation of substances usually trapped near the forest floor. Fitzjarrald et al. (1990). Oliveira et al. (2020) investigated the evolution of turbulence quantities from tall tower micrometeorological observations in four storm events observed during an intensive operating period (IOP) at the Amazon Tall Tower Observatory (ATTO), and found the gust fronts and cold pools can substantially augment the sensible and latent heat fluxes because the cold pool drastically cools and dries the undisturbed (pre-storm) PBL and enhances the winds and the turbulence locally. In a recent study, Mendonça et al. (2023) found that night-time convective downdrafts can fully couple the air flow in the forest air with the overlying PBL in weakly stable regimes. Moreover, some studies have shown that deep convective downdrafts are able to advect ozone-rich air towards the surface and induce peaks in its concentration immediately after gust front passage at a given location (Betts et al., 2002; Dias-Júnior et al., 2017; D'Oliveira et al., 2022; Gerken et al., 2016). Of particular relevance is the study of D'Oliveira et al. (2022), who showed via cloud-resolving numerical simulations of storms in the Amazon that convective downdrafts are less efficient in 'cleaning' the atmosphere of trace gases such as carbon monoxide in situations with abundant fire emissions. More recently, da Silva et al. (2023) have shown that squall line events can engender carbon dioxide (CO₂) enhancements in the Amazon with lifespans within 1–

3 h; the mechanisms that cause such peaks, however, warrant further investigation.

On 27 December 2021, an MCS moved north through the eastern portion of the Amazonas state, northern Brazil, and produced a large and strong gust front. As the MCS decayed during daytime hours, its gust front continued to surge northward and passed the ATTO site, causing large changes in the evolution of thermodynamic, kinematic and chemical properties of the PBL that persisted for several hours. This case is particularly interesting given that the gust front moved north-northeast as in some less frequent windthrow events, but persisted well after the dissipation of the parent MCS. More importantly, this convective system was responsible for significantly enhancing CO₂ concentrations that were well observed by high-frequency measurements at ATTO. This aspect is of chief concern given the key role played by CO₂ as a greenhouse gas in the global carbon, radiation and heat budgets. Understanding the mechanisms that redistribute CO₂ in the atmosphere is crucial for an accurate depiction of the terrestrial carbon sink (Keenan & Williams, 2018), especially when the mechanisms include mesoscale phenomena (Fujita, 1981) such as convective storms, low-level jets and gravity waves (Corrêa et al., 2021), whose roles in redistributing CO₂ have received less attention compared to phenomena on larger (synoptic) scales or smaller (turbulence) scales. Therefore, in this study, we analyse this event to determine the main characteristics of the gust front and its attendant cold pool and to evaluate how they are related to the CO₂ concentration increases observed at ATTO. Emphasis is given to the time-height evolution of thermodynamic, kinematic and CO₂ structures of the gust front in the lower PBL and the possible causes of the CO₂-rich air mass.

The paper is organised as follows. Section 2 describes the micrometeorological measurements at ATTO and the meteorological data employed in the analysis. Section 3 presents the results, including a detailed assessment of the evolution of the gust front and its relationship with the CO₂-rich air mass. A summary and conclusions are provided in Section 4.

2 | DATA AND METHODS

2.1 | Micrometeorological measurements at the Amazon Tall Tower Observatory site

We use micrometeorological data collected at the ATTO site (Dias et al., 2023) to study a gust front that occurred on 27 December 2021 in this region. The ATTO site is

located in a small plateau surrounded by non-flooded upland forest with an average height of 37 m above ground level (a.g.l.; hereafter, all heights are a.g.l.) (Oliveira et al., 2018). The leaf area density profile can be found in figure 2b of Gomes Alves et al. (2023). Data from two towers of ATTO separated by approximately 650 m were evaluated: the 81-m Instant tower located at 2°08.64' S, 58°59.99' W and the 325-m Tall tower located at 2°08.75' S, 58°00.33' W, equipped with thermohygrometers and sonic anemometers designed to measure meteorological quantities to better understand the complex interactions between the Amazon forest and the atmosphere. 3D wind measurements were obtained from sonic anemometers (CSAT3B, Campbell Scientific, Inc.) and CO₂ and water vapour concentrations were measured by a closed-path gas analyser (7200 RS by LI-COR Inc.). We analysed sonic anemometer data from the 5, 25, 50, 75, 82.5, 196.5 and 316.5 m levels and gas analyser measurements at 5, 75, 82.5, 196.5 and 316.5 m, with the 5, 25, 50 m levels located at the Instant tower and the 75, 82.5, 196.5 and 316.5 m levels at the Tall tower. A visual quality control procedure for the Instant tower 25-m and 50-m inlets displayed unrealistic and likely erroneous values of CO₂ and water vapour concentrations for this period with respect to their typical profiles at ATTO. To avoid the possible inclusion of erroneous data, we decided to exclude these heights from our analyses. In addition, comparison of the LICOR-7200 CO₂ concentrations to allocated calibrated CO₂ concentrations in the subsequent year (April 2022) showed a constant offset of ~25 ppm, meaning that the displayed CO₂ concentrations in this study are ~25 ppm below the actual concentrations. The reported CO₂ concentrations are not corrected for this offset. Both the anemometers and gas analysers operate at a 10 Hz frequency. Data from humidity-temperature sensors (I-Series, Galltec + Mela) placed at the 1.5, 26, 36, 55, 73 and 81 m levels of the Instant tower were inspected together with data from a pressure sensor to obtain a more accurate and detailed evolution of the gust front. Horizontal wind from a 2D Wind-Sonic ultrasonic anemometer (Gill Instruments Ltd., UK) at the 73 m level of the Instant tower was evaluated because it provided more continuous and reliable time series of horizontal wind speed and direction during the gust front/cold pool than the 3D anemometers near this level, whose measurements were unreliable due to precipitation. For estimating precipitation intensity, we relied on measurements from an automated tipping bucket rain gauge (ARG100, EMLtd.) available at 81 m.

It is well known that during precipitation, sonic anemometers may drastically lose accuracy and result in low quality, unreliable 3D wind and temperature measurements (Friehe, 1976; Mauder & Zeeman, 2018; Zhang

et al., 2016). Due to the occurrence of precipitation during and after the gust front investigated herein, eddy covariance flux data is unreliable and unfortunately precluded a detailed evaluation of the turbulent fluxes during the gust front and cold pool event. Still, the sonic anemometer data was useful to provide a general picture of the time-height evolution of the horizontal wind speed during the gust front. In processing the sonic anemometer data, we removed the spikes and used 1-min average intervals to remove high-frequency oscillations but also to retain some degree of fine-scale detail that may be relevant to the time-height evolution of the gust front.

Finally, we investigated the potential role played by biomass burning as the cause of CO₂-rich air transported by the gust front. For this purpose, we assessed the total aerosol particle number concentration (N) measured by the condensation particle counter (CPC) at 60 and 325 m inlets at the Instant tower and Tall tower, respectively (Franco et al., 2021; Holanda et al., 2023).

Throughout the article times are Universal Time Coordinated (UTC); for reference, local standard time is UTC – 4. Sunrise and sunset times in central Amazon on 27 December 2021 were 0952 and 2210 UTC, respectively.

2.2 | Meteorological and environmental datasets

Analyses of the mesoscale structure of the gust front were conducted using the visible and enhanced infrared channels of the Geostationary Operational Environmental Satellite 16 (GOES-16) and Doppler radar imagery around the time of the event. The S-band radar is located in Manaus, in the state of Amazonas (3°09'0 S, 59°59'0 W), and is operated by the Brazilian Air Force's Department of Airspace Control (SIPAM/DECEA; acronym in Portuguese). The main features of the radar include its single polarization, beamwidth of 1.8° and 250-km range in short pulse mode. In volume-scan mode, the radar obtains a full set of plan-position indicators (PPIs) at 15 elevations at 10-min intervals. To evaluate the structure of the MCS and its gust front, we used constant PPIs obtained from the maximum values of reflectivity (MAXCAPPI) obtained in the atmospheric column by the Manaus radar (available at <https://www.redemet.aer.mil.br/>).

In order to investigate the possibility of forest fires influencing the properties of the gust front/cold pool air mass, we analysed forest fire data from the public interface BDQueimadas (Setzer et al., 2019) maintained by the Brazilian National Institute of Space Research (INPE; acronym in Portuguese) (available at <http://terrabrasilis.dpi.inpe.br/queimadas/bdqueimadas>).

BDQueimadas comprises a large database of the geographical distribution of forest fire foci detected by a set of onboard satellite sensors. We evaluated the distribution of forest fire foci from 26 through 27 December 2021 overlaid on visible imagery provided by Visible Infrared Imaging Radiometer Suite (VIIRS) aboard the National Oceanic and Atmospheric Administration satellite 20 (NOAA-20) available at BDQueimadas. VIIRS obtains visible and infrared imagery with 22 imaging and radiometric bands covering wavelengths from 0.41 to 12.5 μm.

In addition, we analysed the upper-air sounding released at 1200 UTC on 27 December 2021 at the Manaus airport (SBMN) (available at <https://weather.uwyo.edu/upperair/sounding.html>) to estimate source layers of the air in the cold pool observed at the ATTO towers. This was accomplished by comparing equivalent potential temperature (θ_e) observations at the ATTO towers in the cold pool to the θ_e profile from SBMN. This qualitative analysis is based on previous studies that have estimated air parcel source heights of convective outflow by assuming conservation of θ_e in moist adiabatic descent of convective downdrafts (Betts et al., 2002) and comparing the observed θ_e deficits in cold pools to nearby upper-air profiles of θ_e to determine the layers where the low- θ_e air likely originated.

3 | RESULTS

3.1 | Characteristics of the gust front on the mesoscale and at ATTO

An overall assessment of the evolution of the MCS and its gust front is provided in Figure 1. Figure 1a–c shows GOES-16 enhanced infrared brightness temperature (T_B) at 1200, 1500 and 1800 UTC focused on northern South America to highlight the main areas with active deep convection. At 1200 UTC (Figure 1a), the deepest convective storms were located in northern South America and the most prominent MCS was located along the border between southeastern Amazonas and southwestern Pará states. This MCS developed during the evening of the previous day in an area of strong convective activity in southwestern Pará state (not shown). In the morning, the MCS was still vigorous as noted by its cloud top T_B ranging from –90°C to –80°C (Figure 1a) and by its relatively well-defined leading line, trailing stratiform structure (Houze et al., 1990; Houze Jr, 2004) with high reflectivity (>50 dBZ) along the leading line as observed by the Manaus radar (Figure 1d). By 1500 UTC, the leading edge of the MCS had moved ~100 km north-eastward (~140 km northward) and its intensity decreased

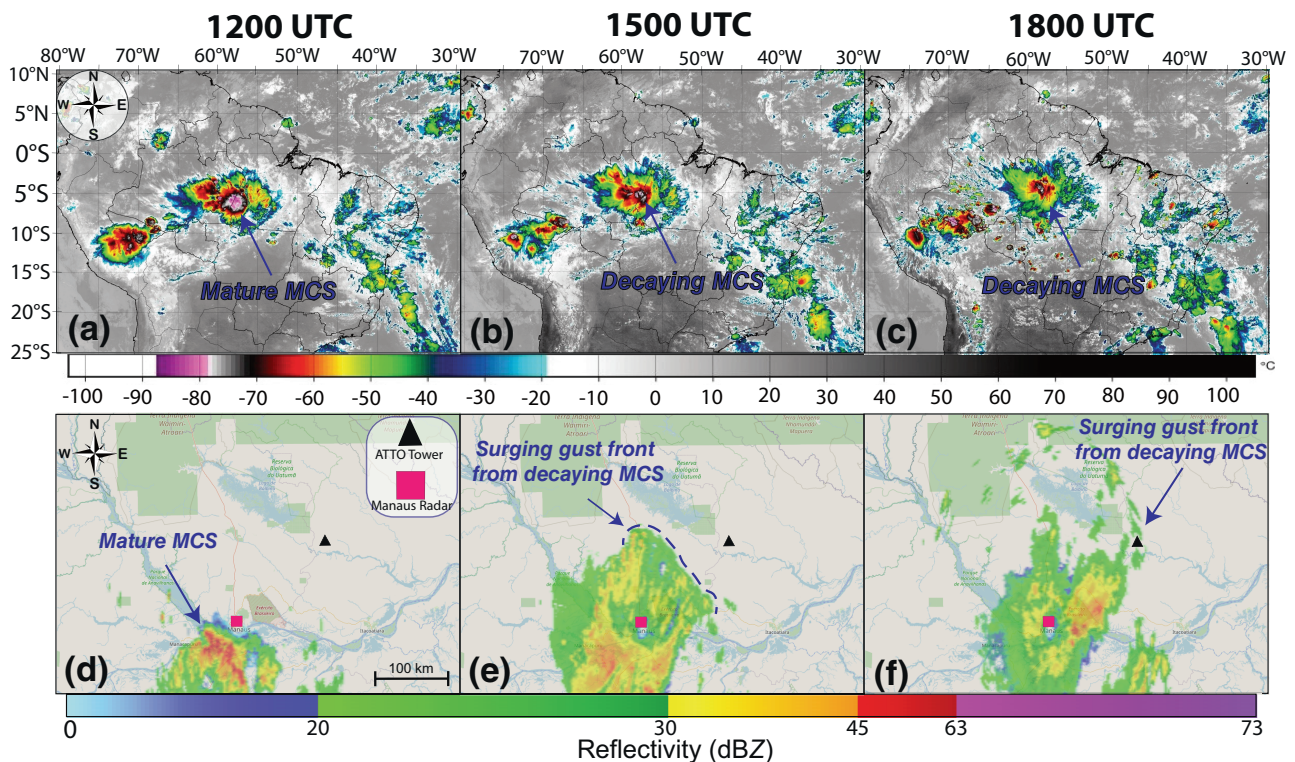


FIGURE 1 (a–c) GOES-16 cloud-top brightness temperature (T_B ; °C) over northern South America. (d–f) MAXCAPPI reflectivity from the Manaus Doppler radar zoomed-in view around the area where the gust front surged northward. The magenta square denotes the location of the Manaus radar and the black triangle denotes the ATTO site. In (e), the dark blue dashed line delineates the approximate location of the surging gust front.

drastically, with its area of $T_B < -80^\circ\text{C}$ reduced to small pockets (Figure 1b) and its reflectivity structure restricted to stratiform precipitation (i.e., reflectivities in the 20–45 dBZ range) (Figure 1e). It is seen in Figure 1e that the northern portion of the precipitation shield (denoted by a blue dashed line) of the MCS began to surge northward. At 1800 UTC, the MCS slightly decreased in size and continued to weaken as noted by the much smaller area with $T_B < -80^\circ\text{C}$ and the general reduced area with $T_B < -55^\circ\text{C}$ (Figure 1c), the latter being a threshold that is often used to detect convectively active regions of MCSs (Machado et al., 1998). The gust front surged farther north/north-eastward and detached from the residual stratiform precipitation shield of the MCS by this time, which is highlighted in Figure 1f as a fine line of weak reflectivities ($\sim 20\text{--}30$ dBZ) several kilometres ahead of the strongest core of the decaying MCS. Based on the Manaus radar observations, the average speed of the gust front towards the northeast was crudely estimated around $35\text{--}40$ km h⁻¹ ($9.1\text{--}11.1$ m s⁻¹). This estimated speed is within the range of gust front propagation speeds found in previous research based on Doppler radar observations (Mahoney, 1988) and numerical simulations based on density current dynamics (Hutson et al., 2019). The overall MCS characteristics described above are consistent with previously documented MCSs

in the Amazon basin, which tend to develop most frequently during late afternoon and evening hours and dissipate during the morning and early afternoon hours of the next day (Bezerra et al., 2021; Machado et al., 2014; Melo et al., 2019). In addition, the structure and evolution of the MCS based on radar data is in agreement with southerly squall line events documented by Negrón-Juárez et al. (2017), who showed that such events typically occur from November to January.

The evolution of 1-min averaged thermodynamic and kinematic quantities measured at the 81-m Instant tower presented in Figure 2 shows that the gust front arrived at the ATTO site around 1600 UTC on 27 December 2021. Before the gust front arrived, the horizontal winds at 73 m (Figure 2a) were predominantly from the northeast ($\sim 30^\circ$) and calm (~ 2 m s⁻¹), which is typical of the Amazon low-level wind regime (Santana et al., 2018). With the arrival of the gust front, the horizontal wind shifted to southwesterlies in consistency to the gust front propagation direction and strengthened to a peak wind speeds within $7\text{--}12$ m s⁻¹ at the gust front, although the winds were stronger aloft, as will be discussed in Section 3.2. The most notable feature of the gust front was the dramatic drop in temperature measured by the thermohygrometer at 81 m (Figure 2b); air temperature dropped approximately 6.5 K from an average 300.5 K in less than

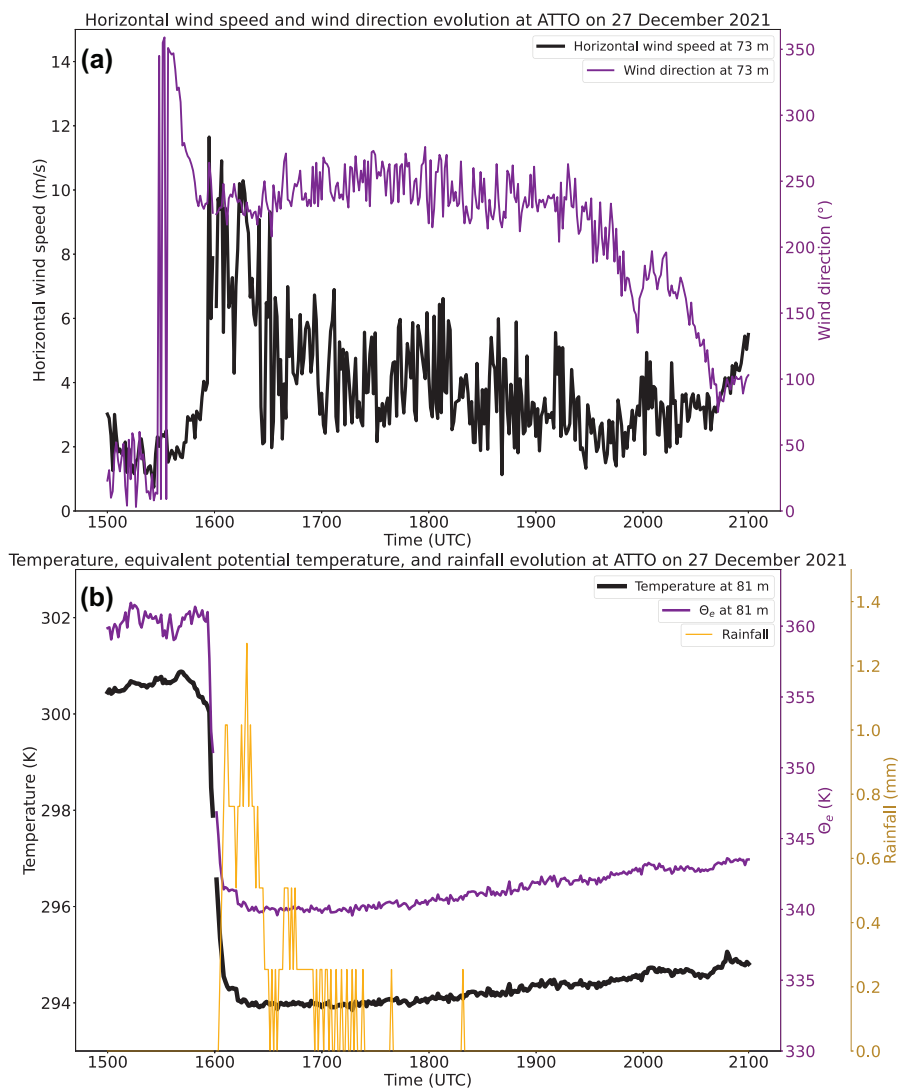


FIGURE 2 1-min-averaged thermodynamic and kinematic fields highlighting the gust front passage and cold pool establishment at the 81-m Instant tower of ATTO. (a) Air temperature (black line; K) and equivalent potential temperature (θ_e , purple line; K) at 81-m and rainfall rate (golden line; mm). (b) Horizontal wind speed (m s^{-1}) and wind direction ($^\circ$) at 73 m.

5 min while θ_e decreased 15–20 K from 360 K to 340–345 K. Such large drops in temperature point to a robust gust front and an attendant strong cold pool that propagates forward as a density current driven by cold, dry air from higher levels (Dias-Júnior et al., 2017; Wakimoto, 1982).

In the cold pool, the wind speed remained enhanced by about 2 m s^{-1} relative to the pre-gust-front values and the wind direction remained from the southwest more than 4 h after the gust front passage (Figure 2a); similarly, the temperature remained well below the pre-gust-front conditions (Figure 2b). The tendency for the air mass to recover from the cold pool to pre-gust-front conditions is slow for the wind speed, which tends to weaken 0.5 m s^{-1} per hour and slightly reduce its westerly component; the tendency is similar for temperature, which tends to slightly increase at a rate of 0.125 K per hour. The slow air mass recovery is another indication of a large and strong cold pool (surmounted by cloud cover) that is able to persist at a given location for a long period.

Given that the gust front occurred during the mid-afternoon hours and was strong enough to persist for several hours, air mass recovery near and after sunset is, of course, not expected given the cessation of radiative heating and the inversion of the sensible heat flux at sunset.

The detached nature of the gust front can also be noted in Figure 2b in terms of 1-min rainfall rates. Upon arrival of the gust front at ATTO and in the subsequent 30 min, rainfall rates were generally within 0.8–1.3 mm, which are not particularly high. In the cold pool in the next 1 h (until 1730 UTC), rainfall was slight around 0.2–0.5 mm and became even weaker or absent for the remainder of the cold pool. The lack of heavy precipitation associated with this gust front and cold pool system is a consequence of the gust front surging ahead of the decaying MCS as shown in Figure 1d–f. As the MCS decayed near the Manaus region within 100–150 km southwest of ATTO, its gust front continued to surge northward due to its strong buoyancy deficits in the cold pool (Figure 2b) without a leading line, trailing stratiform

Time-height evolution of V_h , q_v , T , and CO_2 and the total aerosol particle number concentration (N) at 60 m and 325 m -- 27 December 2021

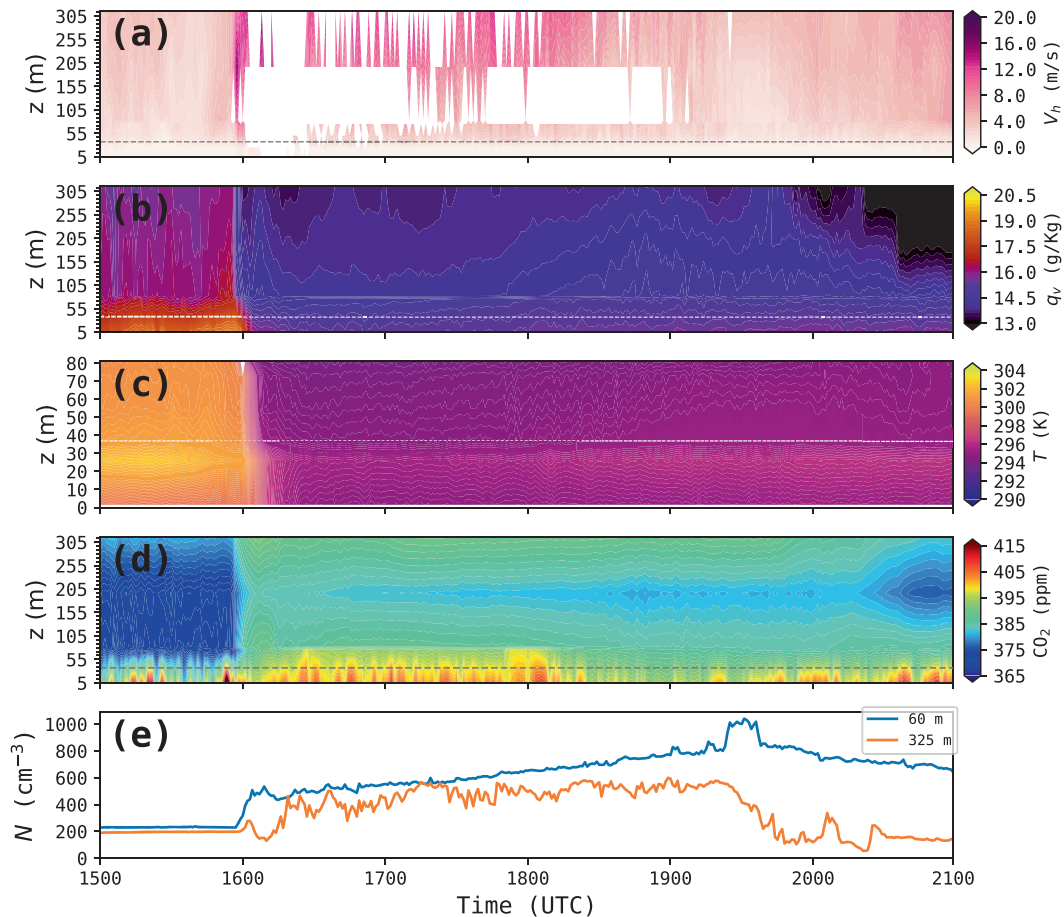


FIGURE 3 Time-height evolution of 1-min-averaged (a) horizontal wind speed (V_h ; m s^{-1}), (b) water vapour mixing ratio (q_v ; g kg^{-1}), (c) temperature (T ; K), and (d) CO_2 concentration (ppm). Time-height plots (a–d) span the depth of the Tall tower (325 m) while (c) is restricted to the time-height evolution of temperature measurements from the thermohygrometers at the Instant tower (81 m). In addition, (e) shows the evolution of particle aerosol concentration (N ; cm^{-3}) measured at the 60 and 325 m levels of the Tall tower. The white/grey lines in (a–d) indicates the mean height of the canopy (37 m).

structure of a mature squall line and was only able to develop weak showers along the gust front. It should be mentioned that, despite relatively weak rainfall, the rainfall rate shown in Figure 2b was sufficient to render the high-frequency (flux) measurements unreliable at most levels of the ATTO tower and precluded detailed analysis of turbulent fluxes during this event. This effect may have been reinforced by the enhanced gust front winds impinging at the sensors.

3.2 | Time-height evolution of wind speed, humidity, temperature and CO_2 concentration during the gust front

Now that the main structural features of the gust front and attendant cold pool have been discussed, we

take a closer look into the time-height evolution of the horizontal wind speed (V_h), water vapour mixing ratio (q_v), temperature (T) and CO_2 concentration at the Tall and Instant towers of ATTO (Figure 3). Through this analysis we can highlight additional relevant and interesting features caused by the 27 December 2021 surging gust front and unravel their likely causes.

First, we investigate the time-height evolution of the V_h based on sonic anemometer data (Figure 3a). The data-void regions in Figure 3a denote periods where the sonic anemometers did not operate properly likely due to rainfall, as discussed in Sections 2.1 and 3.1. Despite the data gaps, the arrival of the gust front at ATTO is evident in Figure 3a when V_h increases above 8 m s^{-1} at all tower levels from 25 through 316.5 m. At the nose of the gust front around 196.5 m, V_h was stronger $\sim 16 \text{ m s}^{-1}$, which suggests a jet-like feature that is

typical of gust fronts (Dias-Júnior et al., 2017). Figure 3a further highlights the persistence of the cold pool at ATTO and shows that V_h values in excess of 12 m s^{-1} persisted at least until 1800 UTC above 150 m and $V_h > 4 \text{ m s}^{-1}$ above the canopy (on average 37 m) until 2000 UTC, despite being very intermittent. Oliveira et al. (2020) have discussed the role played by the strong gust front and cold pool winds in enhancing turbulence and mixing based on eddy covariance flux measurements above and within the forest. Unfortunately, the previously mentioned issues in the high-frequency sonic anemometer measurements precluded a reliable analysis of the eddy covariance fluxes during the event, so an assessment similar to that of Oliveira et al. (2020) was not possible.

Figure 3b,c shows that q_v and T decreased nearly simultaneously through the Instant and Tall towers upon the arrival of the gust front, except for the layer within the canopy where the effects of the gust front lagged those aloft, although such lag is small ($< 5 \text{ min}$) (also notice the different height scales in Figure 3b,c). On one hand, this behaviour is somewhat expected since the dense forest tends to delay and damp to some extent the penetration of convective outflow through the canopy (Oliveira et al., 2020); on the other hand, the small lag time corroborates the strength of the gust front and its capacity to disturb the air mass inside the forest (Fitzjarrald et al., 1990). Above 82.5 m, q_v decreased from 17.5 g kg^{-1} to 13.5 g kg^{-1} while within the forest (i.e., at the 5 m level) it decreased from 19 g kg^{-1} to 15 g kg^{-1} . In spite of the differences among measurement levels, the drying in the cold pool is consistent with the water vapour deficits caused in tropical deep convective downdrafts [e.g., the $3\text{--}4 \text{ g kg}^{-1}$ reported by Johnson & Nicholls, 1983]. Figure 3c also illustrates that, in spite of the penetration of cold outflow air towards the forest lower levels, the overall structure of the semi-permanent stable layer below the canopy persists.

The cooling and drying presented in Figure 3b,c are consistent with the $15\text{--}20 \text{ K}$ drop in θ_e deficits in the cold pool discussed in Figure 2b. A closer inspection of the θ_e deficits can indicate the source height of the air composing the cold pool by comparing them to the θ_e profile obtained from 1200 UTC on 27 December 2021 sounding at the Manaus airport (SBMN). Before analysing the profile, we must stress three potential issues that can affect the interpretation of our results. First, the sounding was taken 4 h before the arrival of the gust front at ATTO and 150 km away from the ATTO site. Thus, we assume the large-scale environment downstream from the MCS is relatively homogeneous and we assume semi-stationary conditions above the PBL. Second, the SBMN sounding was released just before the arrival of the mature MCS at

Manaus (Figure 1d–f), which may have resulted in some degree of convective contamination. Third, we assume relatively weak diabatic heating during the horizontal parcel excursions from the base of the downdraft through the gust front; this assumption is reasonable because the thick cloud shield of the MCS persisted throughout the day and damped radiative heating. Based on our assessment of the sounding, we deem the θ_e profile sufficiently representative of the large-scale vertical distribution of θ_e at least qualitatively, but we acknowledge that the sounding does not represent a true proximity sounding (Potvin et al., 2010). Keeping these caveats in mind, we now analyse the vertical profile of θ_e at SBMN in Figure 4. The θ_e deficits in Figure 2b are consistent with air parcels that have descended from two layers; a mid-level layer from 2.4 to 5.3 km and an upper-level layer from 7.4 to 9.1 km. Given that the profile was obtained close to the MCS when it was mature, air from both layers may have been part of the outflow observed at the towers because at this stage the MCS was more likely to produce large, deep and relatively undiluted downdrafts. Yet, using a similar methodology, Betts et al. (2002) have found that downdrafts in the Amazon rainforest tend to form just above cloud base in consistency with the mid-level layer found in this study, a result that is supported by previous research (Betts, 1976). Hence, it seems plausible that the air parcels composing the cold pool in this study originated predominantly from the mid-level layer.

We now turn our attention to the time-height evolution of the CO_2 concentration in the gust front and cold pool (Figure 3d). The arrival of the gust front at the ATTO towers is marked by a sudden increase in CO_2 concentration at all levels. CO_2 concentrations, which were already high within and just above the forest canopy before the gust front, rapidly increased and deepened after the gust front passage with values as high as 395–415 ppm which were originally confined to the lowest data level (5 m) reaching as high as 82.5 m from 1600 to 1800 UTC. Above the 82.5 m, CO_2 concentrations also increased notably, rising 5–15 ppm from the pre-gust-front values of around 370–380 ppm. As with the time-height evolution of V_h and q_v , that also changed nearly simultaneously over most tower levels, it is clear that horizontal advection of CO_2 from a region of high CO_2 concentration upstream occurred and was caused by the gust front. Before addressing the potential cause of the CO_2 -rich air mass, it is interesting to note that the pre-gust-front elevated CO_2 concentrations within the forest canopy relative to the above canopy values stand in contrast with typical profiles of CO_2 in the Amazon forest which increase with heights due to photosynthesis in the forest (Wofsy et al., 1988). The high in-canopy CO_2 values observed in Figure 3d may be a result

of thick cloud cover from the decaying MCS cirrus shield preceding the gust front. The thick cloud cover acted to reduce the amount of incoming shortwave radiation and photosynthesis rates within and near forest canopy, consequently and drastically reducing the sequestration of CO_2 by the forest before the gust front.

Finally, we attempt to determine the cause of the CO_2 -rich air carried by the gust front towards the ATTO site. It is well-established that storms in the Amazon can locally increase concentrations of some chemical species such as ozone by transporting ozone-rich air from the upper troposphere and lower stratosphere to the surface via deep downdrafts (Betts et al., 2002; Gerken et al., 2016). Considering that typical profiles of CO_2 above the Amazon forest show decreasing values of CO_2 concentration with height because of photosynthesis, especially in the absence of cloud cover (Bertani et al., 2017; Graham et al., 2003; Green et al., 2020), one may presume that the CO_2 jump presented in Figure 3d occurred, at least partially, due this vertical advection process. This reasoning is consistent with the θ_e analysis, which showed potential air parcel sources heights from low and upper levels (Figure 4) and is also consistent with a peak in ozone observed during this event (not shown). However, another possible and more remarkable source for the CO_2 -rich air is the occurrence of biomass burning upstream from the ATTO site (Jiang et al., 2021). This hypothesis has support in Figure 5, which shows satellite-detected fire foci from 26 to 27 December in the Amazon and surrounding areas. Several fire foci can be seen in Figure 5, but the most notable ones are located

within 50–100 km south of the ATTO site and stretch towards and south of Manaus. Given that the gust front moved from the southwest (the area where the fires were occurred) to the northeast towards the ATTO site (Figures 1 and 2a), it is reasonable to presume that smoke from biomass burning contributed significantly to the high CO_2 concentration that was advected northward by the gust front and observed at ATTO. This possibility is substantiated by CPC measurements obtained at 60 and 325 m at the ATTO towers (Figure 3e), which show aerosol concentrations increasing abruptly around 1600 UTC during the arrival of the gust front at ATTO. For this event, unfortunately, carbon monoxide measurements, which are often used to more clearly indicate biomass burning (Dajti et al., 2024), were not available. Figure 3e shows that the initial increase in aerosol concentration is more noticeable at 60 m, increasing from pre-gust-front concentrations of 210 to 550 cm^{-3} , later steadily increasing to values in excess of 1000 cm^{-3} . At 325 m, the initial increase to N around 400 cm^{-3} is delayed by 10 min from the early peak observed at 60 m, but the same increasing trend over time during the span of the cold pool exists, since the two towers are located 650 m away from each other. Large reductions in aerosol concentration occur much later at 325 m and more slowly at 60 m as a result of the onset of dissipation of the cold pool at ATTO. Therefore, the behaviour of the aerosol measurements provides evidence that the high CO_2 concentrations observed at the ATTO site on 27 December 2021 may have contributions from biomass burning, which were later transported northward by the mesoscale flow of the gust front. Further contributions to the CO_2 and aerosol increases may have occurred due to storm processes other than horizontal advection by the gust front. Such processes include non-local mixing caused by vertical advection by convective downdrafts which often transport fine-scale particles towards the surface (Franco et al., 2024; Wang et al., 2016) and local mixing caused by the interaction of gust front and the topography surrounding ATTO.

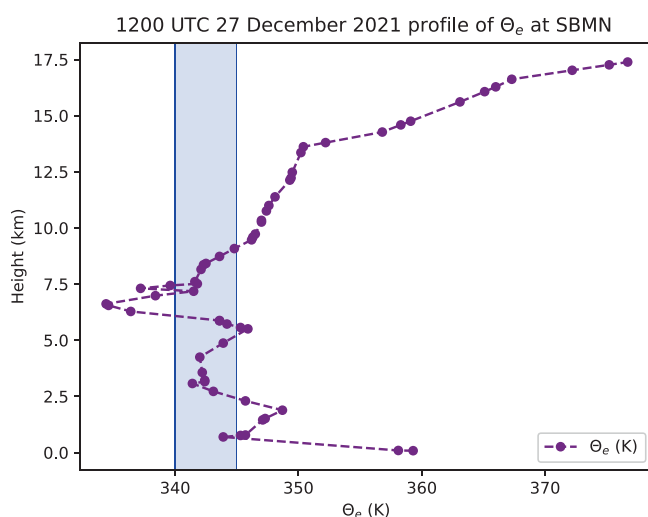


FIGURE 4 Vertical profile of θ_e (K) at 1200 UTC on 27 December 2021 from the SBMN upper-air station (purple line). The vertical shaded area delineates the layer within the 340–345 K range discussed in the text.

4 | CONCLUSIONS

This study investigated the occurrence of a strong, northward surging gust front at ATTO on 27 December 2021. This event was especially important because it was reminiscent of northward surging squall lines, which are rarer than the typical northeasterly squall lines that impact central Amazon. The gust front was produced by a decaying mesoscale convective system that formed on the previous day and moved north along the Amazonas-Pará state border and was responsible for abrupt changes in the evolution of thermodynamic, kinematic and chemical

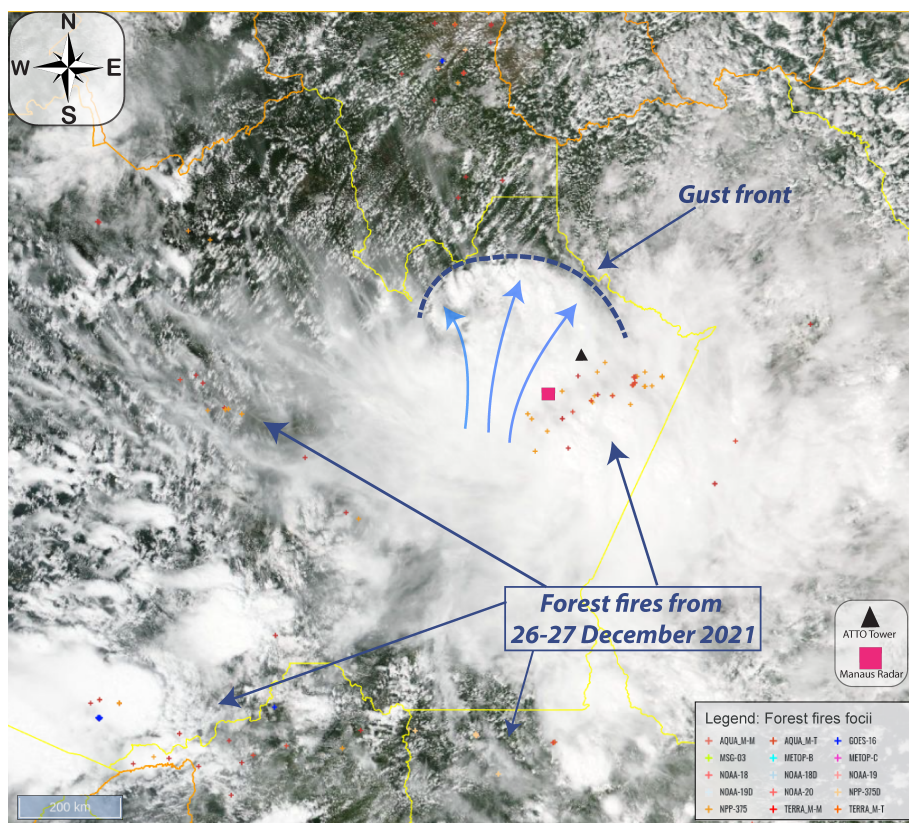


FIGURE 5 NOAA-20 visible imagery centered on the Amazon region. Forest fire foci from 26 through 27 December 2021 detected by environmental satellites and compiled by BDQueimadas (INPE) are denoted by the colored diamond symbols at the bottom right portion of the figure. The dark blue dashed line delineates the approximate location of the surging gust front. The light blue curved arrows illustrate the inferred horizontal flow behind the gust front.

properties of the lower boundary layer at the ATTO site. The large temperature drop and strong winds at the tall towers suggest that the gust front surged northward as a result of density current dynamics, as expected from theory and the lack of synoptic-scale forcing. The temperature and wind disturbances persisted for several hours at the towers, emphasizing that the cold pool behind the gust front was large and strong.

The strong cooling and drying observed at ATTO resulted in θ_e deficits of 15–20 K in the cold pool. A comparison of θ_e computed from measurements at the Instant tower with the θ_e profile obtained at 1200 UTC on 27 December 2021 profile of θ_e at Manaus suggests that air parcels composing the cold pool at and behind the gust front descended from mid-level altitudes (2.4–5.3 km), which is consistent with past literature, although the downdrafts could have originated, at least partially, from layers as high as 6–9 km AGL.

The result of main relevance was the abrupt increase of CO_2 concentration through the depth of the measurements. Such increase was caused by horizontal advection of CO_2 by the gust front from an area upstream of the ATTO rich in CO_2 . Although some of the CO_2 could be due to downward transport and horizontal transport of CO_2 -rich air from above the photosynthetically active portion of the forest, a more remarkable source for the CO_2 is the occurrence of biomass burning upstream from

ATTO detected by satellite on 26 and 27 December 2021. This hypothesis is supported by condensation particle counter measurements at the tall towers, which showed jumps in aerosol concentrations concomitant with the onset of the gust front, which also lasted during the lifespan of the cold pool at the ATTO site, although we note that such jumps in aerosol concentrations can be caused by downward advection of fine-scale particles in the cold pool. Regardless, this result is key because it underscores the role played by mesoscale convective flows in redistributing CO_2 (as well as other trace gases) in the Amazon forest and its consequences in modulating the carbon cycle and greenhouse effect across distant parts of the forest on the order of 100–500 km. Such convectively induced transport of trace gases across the Amazon may be relatively common during the dry season when biomass burning is more widespread despite reduced frequency and coverage of deep convection. This topic should be further investigated in future studies for larger samples of storm cases, especially during the dry season of the Amazon, when forest fires are more common. Although much has been learned from the transport of smoke from biomass burning on micro and macro (synoptic) scales, little research has been conducted to analyse the role played by convectively induced mesoscale flows in that transport. In this sense, another avenue for research could employ cloud-resolving numerical

simulations of storms in the Amazon to address the mechanisms by which the storms and associated outflow transport and disperse trace gases from forest fires. By employing such tools, one can track air parcel motions to accurately determine outflow source regions and determine the budgets of trace gases as outflows redistribute them across different portions of the Amazon forest.

AUTHOR CONTRIBUTIONS

Luciane I. Reis: Conceptualization; investigation; writing – original draft; methodology; software; formal analysis; visualization; writing – review and editing; validation. **Maurício I. Oliveira:** Conceptualization; investigation; writing – original draft; writing – review and editing; formal analysis; visualization; supervision; methodology; validation. **Cléo Q. Dias-Júnior:** Funding acquisition; writing – review and editing; project administration; investigation; supervision; resources; formal analysis. **Hella van Asperen:** Investigation; writing – review and editing; formal analysis; validation; data curation. **Luca Mortarini:** Investigation; writing – review and editing; validation; data curation. **Otávio C. Acevedo:** Writing – review and editing; investigation. **Christopher Pöhlker:** Writing – review and editing; validation. **Leslie A. Krempfer:** Data curation; writing – review and editing; validation. **Bruno Takeshi:** Data curation; resources. **Carlos A. Quesada:** Data curation; resources; funding acquisition. **Daiane V. Brondani:** Investigation; writing – review and editing; data curation.

ACKNOWLEDGEMENTS

We thank the Instituto Nacional de Pesquisas da Amazônia (INPA) and the Max-Planck Society for continuous support. We acknowledge the support by the German Federal Ministry of Education and Research (BMBF contract 01LB1001A, 01LK1602A, 01LK1602B, and 01LK2101) and the Brazilian Ministério da Ciência, Tecnologia e Inovação (MCTI/FINEP contract 01.11.01248.00) as well as the Amazon State University (UEA), FAPEAM, CAPES and SDS/CEUC/RDS-Uatumã. Cléo Q. Dias-Júnior acknowledges support from CNPQ (Processes 440170/2022-2, 406884/2022-6, 307530/2022-1). We also thank all the field assistants and personnel involved in the support of the ATTO project.

CONFLICT OF INTEREST STATEMENT

None of the authors have a conflict of interest to disclose.

DATA AVAILABILITY STATEMENT

The data that support the findings of this study are available from the corresponding author upon reasonable request.

ORCID

Luciane I. Reis  <https://orcid.org/0009-0007-6717-862X>

Maurício I. Oliveira  <https://orcid.org/0000-0002-9388-2334>

Cléo Q. Dias-Júnior  <https://orcid.org/0000-0003-4783-4689>

Luca Mortarini  <https://orcid.org/0000-0002-0543-2975>

Daiane V. Brondani  <https://orcid.org/0000-0002-7197-8618>

REFERENCES

- Alcântara, C.R., Dias, M.A.S., Souza, E.P. & Cohen, J.C. (2011) Verification of the role of the low level jets in amazon squall lines. *Atmospheric Research*, 100, 36–44.
- Alonso, M.F. & Saraiva, J. (2005) Simulation of a squall line occurred in january 18th 2005. In proceedings of the international symposium on Nowcasting and very short range forecasting (WSN05), 8, 28.
- Bertani, G., Wagner, F.H., Anderson, L.O. & Aragão, L.E. (2017) Chlorophyll fluorescence data reveals climate-related photosynthesis seasonality in amazonian forests. *Remote Sensing*, 9, 1275.
- Betts, A.K. (1976) The thermodynamic transformation of the tropical subcloud layer by precipitation and downdrafts. *Journal of Atmospheric Sciences*, 33, 1008–1020.
- Betts, A.K., Gatti, L.V., Cordova, A.M., Silva Dias, M.A. & Fuentes, J.D. (2002) Transport of ozone to the surface by convective downdrafts at night. *Journal of Geophysical Research: Atmospheres*, 107, LBA–13.
- Bezerra, V.L., Dias-Júnior, C.Q., Vale, R.S., Santana, R.A., Bota, S., Manzi, A.O. et al. (2021) Near-surface atmospheric turbulence in the presence of a squall line above a forested and deforested region in the central amazon. *Atmosphere*, 12, 461.
- Cohen, J.C., Silva Dias, M.A. & Nobre, C.A. (1995) Environmental conditions associated with amazonian squall lines: a case study. *Monthly Weather Review*, 123, 3163–3174.
- Corrêa, P.B., Dias-Júnior, C.Q., Cava, D., Sörgel, M., Bota, S., Acevedo, O. et al. (2021) A case study of a gravity wave induced by amazon forest orography and low level jet generation. *Agricultural and Forest Meteorology*, 307, 108457.
- da Silva, G.H.S., Dias-Júnior, C.Q., Cohen, J.C.P. & Wolff, S. (2023) Squall line in the amazon region and the transport of gas near the surface during the occurrence of downdraft. *Ciência E Natura*, 45, e81657.
- Dajti, G., Urquiza, D., van Asperen, H., Jones, S., Komiya, S., Lavric, J. et al. (2024) Fire trends on atto footprint over the last two decades. Tech. rep., Copernicus Meetings.
- Dias, N.L., Toro, I.M.C., Dias-Júnior, C.Q., Mortarini, L. & Brondani, D. (2023) The relaxed eddy accumulation method over the amazon forest: the importance of flux strength on individual and aggregated flux estimates. *Boundary-Layer Meteorology*, 189, 139–161.
- Dias-Júnior, C.Q., Dias, N.L., Fuentes, J.D. & Chamecki, M. (2017) Convective storms and non-classical low-level jets during high ozone level episodes in the amazon region: an arm/goamazon case study. *Atmospheric Environment*, 155, 199–209.
- D'Oliveira, F.A., Cohen, J.C., Spracklen, D.V., Medeiros, A.S., Cirino, G.G., Artaxo, P. et al. (2022) Simulation of the effects of

- biomass burning in a mesoscale convective system in the central amazon. *Atmospheric Research*, 278, 106345.
- Fitzjarrald, D.R., Moore, K.E., Cabral, O.M., Scolar, J., Manzi, A.O. & de Abreu Sá, L.D. (1990) Daytime turbulent exchange between the amazon forest and the atmosphere. *Journal of Geophysical Research: Atmospheres*, 95, 16825–16838.
- Fournier, M.B. & Haerter, J.O. (2019) Tracking the gust fronts of convective cold pools. *Journal of Geophysical Research: Atmospheres*, 124, 11103–11117.
- Franco, M.A., Ditas, F., Kremper, L.A., Machado, L.A., Andreae, M.O., Araújo, A. et al. (2021) Occurrence and growth of sub-50 nm aerosol particles in the amazonian boundary layer. *Atmospheric Chemistry and Physics Discussions*, 2021, 1–36.
- Franco, M.A., Valiati, R., Holanda, B.A., Meller, B.B., Kremper, L.A., Rizzo, L.V. et al. (2024) Vertically resolved aerosol variability at the amazon tall tower observatory under wet season conditions.
- Friehe, C.A. (1976) Effects of sound speed fluctuations on sonic anemometer measurements. *Journal of Applied Meteorology*, 1962-1982, 607–610.
- Fujita, T.T. (1981) Tornadoes and downbursts in the context of generalized planetary scales. *Journal of Atmospheric Sciences*, 38, 1511–1534.
- Garstang, M., Massie, H.L., Halverson, J., Greco, S. & Scala, J. (1994) Amazon coastal squall lines. Part i: structure and kinematics. *Monthly Weather Review*, 122, 608–622.
- Gerken, T., Wei, D., Chase, R.J., Fuentes, J.D., Schumacher, C., Machado, L.A. et al. (2016) Downward transport of ozone rich air and implications for atmospheric chemistry in the amazon rainforest. *Atmospheric Environment*, 124, 64–76.
- Gomes Alves, E., Aquino Santana, R., Quaresma Dias-Júnior, C., Bota, S., Taylor, T., Yáñez-Serrano, A.M. et al. (2023) Intra-and interannual changes in isoprene emission from central amazonia. *Atmospheric Chemistry and Physics*, 23, 8149–8168.
- Graham, E.A., Mulkey, S.S., Kitajima, K., Phillips, N.G. & Wright, S.J. (2003) Cloud cover limits net co₂ uptake and growth of a rainforest tree during tropical rainy seasons. *Proceedings of the National Academy of Sciences*, 100, 572–576.
- Greco, S., Scala, J., Halverson, J., Massie, H.L., Tao, W.-K. & Garstang, M. (1994) Amazon coastal squall lines. Part ii: heat and moisture transports. *Monthly Weather Review*, 122, 623–635.
- Green, J., Berry, J., Ciais, P., Zhang, Y. & Gentine, P. (2020) Amazon rainforest photosynthesis increases in response to atmospheric dryness. *Science Advances*, 6, eabb7232.
- Holanda, B.A., Franco, M.A., Walter, D., Artaxo, P., Carbone, S., Cheng, Y. et al. (2023) African biomass burning affects aerosol cycling over the amazon. *Communications Earth & Environment*, 4, 154.
- Houze, R.A., Jr. (2004) Mesoscale convective systems. *Reviews of Geophysics*, 42, RG4003. doi:[10.1029/2004RG000150](https://doi.org/10.1029/2004RG000150)
- Houze, R.A., Smull, B.F. & Dodge, P. (1990) Mesoscale organization of springtime rainstorms in oklahoma. *Monthly Weather Review*, 118, 613–654.
- Hutson, A., Weiss, C. & Bryan, G. (2019) Using the translation speed and vertical structure of gust fronts to infer buoyancy deficits within thunderstorm outflow. *Monthly Weather Review*, 147, 3575–3594.
- Jiang, X., Li, K.-F., Liang, M.-C. & Yung, Y.L. (2021) Impact of amazonian fires on atmospheric co₂. *Geophysical Research Letters*, 48, e2020GL091875.
- Johnson, R.H. & Nicholls, M.E. (1983) A composite analysis of the boundary layer accompanying a tropical squall line. *Monthly Weather Review*, 111, 308–319.
- Keenan, T. & Williams, C. (2018) The terrestrial carbon sink. *Annual Review of Environment and Resources*, 43, 219–243.
- Machado, L., Rossow, W., Guedes, R. & Walker, A. (1998) Life cycle variations of mesoscale convective systems over the americas. *Monthly Weather Review*, 126, 1630–1654.
- Machado, L.A., Dias, M.A.S., Morales, C., Fisch, G., Vila, D., Albrecht, R. et al. (2014) The chuva project: how does convection vary across Brazil? *Bulletin of the American Meteorological Society*, 95, 1365–1380.
- Mahoney, W.P. (1988) Gust front characteristics and the kinematics associated with interacting thunderstorm outflows. *Monthly Weather Review*, 116, 1474–1492.
- Mauder, M. & Zeeman, M.J. (2018) Field intercomparison of prevailing sonic anemometers. *Atmospheric Measurement Techniques*, 11, 249–263.
- Melo, A.M., Dias-Júnior, C.Q., Cohen, J.C., Sá, L.D., Cattanio, J.H. & Kuhn, P.A. (2019) Ozone transport and thermodynamics during the passage of squall line in central amazon. *Atmospheric Environment*, 206, 132–143.
- Mendonça, A.C., Dias-Júnior, C.Q., Acevedo, O.C., Santana, R.A., Costa, F.D., Negrón-Juarez, R.I. et al. (2023) Turbulence regimes in the nocturnal roughness sublayer: interaction with deep convection and tree mortality in the amazon. *Agricultural and Forest Meteorology*, 339, 109526.
- Negrón-Juárez, R.I., Jenkins, H.S., Raupp, C.F., Riley, W.J., Kueppers, L.M., Magnabosco Marra, D. et al. (2017) Windthrow variability in central amazonia. *Atmosphere*, 8, 28.
- Oliveira, M.I., Acevedo, O.C., Sörgel, M., Nascimento, E.L., Manzi, A.O., Oliveira, P.E. et al. (2020) Planetary boundary layer evolution over the amazon rainforest in episodes of deep moist convection at the amazon tall tower observatory. *Atmospheric Chemistry and Physics*, 20, 15–27.
- Oliveira, P.E., Acevedo, O.C., Sörgel, M., Tsokankunku, A., Wolff, S., Araújo, A.C. et al. (2018) Nighttime wind and scalar variability within and above an amazonian canopy. *Atmospheric Chemistry and Physics*, 18, 3083–3099.
- Pereira Filho, A.J., Silva Dias, M.A., Albrecht, R.I., Pereira, L.G., Gandu, A.W., Massambani, O. et al. (2002) Multisensor analysis of a squall line in the amazon region. *Journal of Geophysical Research: Atmospheres*, 107, LBA–52.
- Potvin, C.K., Elmore, K.L. & Weiss, S.J. (2010) Assessing the impacts of proximity sounding criteria on the climatology of significant tornado environments. *Weather and Forecasting*, 25, 921–930.
- Rehbein, A., Ambrizzi, T., Mechoso, C.R., Espinosa, S.A. & Myers, T.A. (2019) Mesoscale convective systems over the amazon basin: the goamazon2014/5 program. *International Journal of Climatology*, 39, 5599–5618.
- Santana, R.A., Dias-Júnior, C.Q., da Silva, J.T., Fuentes, J.D., do Vale, R.S., Alves, E.G. et al. (2018) Air turbulence characteristics at multiple sites in and above the amazon rainforest canopy. *Agricultural and Forest Meteorology*, 260, 41–54.
- Setzer, A., Morelli, F. & Souza, J.C. (2019) O banco de dados de queimadas do inpe. *Biodiversidade Brasileira*, 9, 239.

- Wakimoto, R.M. (1982) The life cycle of thunderstorm gust fronts as viewed with doppler radar and rawinsonde data. *Monthly Weather Review*, 110, 1060–1082.
- Wang, J., Krejci, R., Giangrande, S., Kuang, C., Barbosa, H.M., Brito, J. et al. (2016) Amazon boundary layer aerosol concentration sustained by vertical transport during rainfall. *Nature*, 539, 416–419.
- Wofsy, S.C., Harriss, R.C. & Kaplan, W.A. (1988) Carbon dioxide in the atmosphere over the amazon basin. *Journal of Geophysical Research: Atmospheres*, 93, 1377–1387.
- Xie, J., Lan, C., Yang, H., Gao, R., Lu, C., Wang, B. et al. (2022) Tower-observed structural evolution of the low-level boundary layer before, during, and after gust front passage in a coastal area at low latitude. *Weather and Climate Extremes*, 36, 100429.
- Zhang, R., Huang, J., Wang, X., Zhang, J.A. & Huang, F. (2016) Effects of precipitation on sonic anemometer measurements of

turbulent fluxes in the atmospheric surface layer. *Journal of Ocean University of China*, 15, 389–398.

How to cite this article: Reis, L. I., Oliveira, M. I., Dias-Júnior, C. Q., van Asperen, H., Mortarini, L., Acevedo, O. C., Pöhlker, C., Kremper, L. A., Takeshi, B., Quesada, C. A., & Brondani, D. V. (2024). Tall tower observations of a northward surging gust front in central Amazon and its role in the mesoscale transport of carbon dioxide. *Meteorological Applications*, 31(5), e70002. <https://doi.org/10.1002/met.70002>